Solar-Terrestrial Physics. 2025, vol. 11, iss. 2, pp. 78–87. DOI: 10.12737/stp-112202508 © 2025
O.S. Zorkaltseva, O.Yu. Antokhina, A.V. Gochakov, M.F. Artamonov. Published by INFRA-M Academic Publishing House

DOI: 10.12737/stp-112202508

Received January 20, 2025
Accepted March 18, 2025

EVOLUTION OF THE STRATOSPHERIC POLAR VORTEX AS EVIDENCED BY THE WINTERS 2022–2024

O.S. Zorkaltseva
Institute of Solar-Terrestrial Physics SB RAS, Irkutsk, Russia, olgak@iszf.irk.ru

O.Yu. Antokhina
Institute of Solar-Terrestrial Physics SB RAS, Irkutsk, Russia, olgayumarchenko@gmail.com
V.E. Zuev Institute of Atmospheric Optics SB RAS, Tomsk, Russia

A.V. Gochakov
V.E. Zuev Institute of Atmospheric Optics SB RAS, Tomsk, Russia, wandering@bk.ru
Siberian Regional Research Hydrometeorological Institute, Novosibirsk, Russia

M.F. Artamonov
Institute of Solar-Terrestrial Physics SB RAS, Irkutsk, Russia, artamonov.maksim@iszf.irk.ru

Abstract. The paper examines the variation in the stratospheric polar vortex (SPV) area and the high-latitude stratosphere temperature from November to March for the winter periods 2022–2023 and 2023–2024 against the background of average long-term values of these parameters from 1979 to 2024. In 2022–2023, the SPV area significantly exceeded the climatic values in January and December, and a decrease in the SPV area occurred a month later than the climatic normal. This was accompanied by extremely low temperatures in the polar stratosphere in the first half of winter and a record-breaking "hot" sudden stratospheric warming (SSW) in the second half of winter. In the winter period 2023–2024, no extreme SPV and temperature values were observed, but four SSW episodes were recorded during the winter period, three of which were major. We analyze SPV areas, temperatures in the stratosphere, activity of planetary waves, and discuss the reasons for the differences between the two winter seasons in terms of wave activity.

Keywords: stratospheric polar vortex area, sudden stratospheric warmings, planetary waves, wave activity flux.

INTRODUCTION

With the end of summer, a stratospheric polar vortex (SPV) is formed in the Northern Hemisphere, its area increases, and the stratosphere temperature goes down as the inflow of solar radiation to high latitudes decreases. SPV is a cyclonic structure surrounded by powerful westerly winds, which helps to isolate cold air masses in the polar region. In spring, as inflow of solar radiation increases, SPV weakens, its area decreases, the stratosphere temperature rises, and circulation changes direction to the east.

Intraseasonal variability in SPV is characterized by alternating strong and weak vortex events. A strong vortex event is associated with an increase in the vortex area and a decrease in the temperature of the air masses involved in it, which are accompanied by an increase in the westerly flow. During a weak vortex event, the vortex area decreases and temperature rises at high latitudes [Baldwin et al., 2021; Limpasuvan et al., 2005]. These events depend on the interaction of SPV with planetary waves that arise in the troposphere under the influence of orography and temperature contrasts between land and ocean [Andrews et al., 1987]. The interaction of waves with the zonal flow contributes to the formation of stratospheric anticyclones such as Aleutian and European. These anticyclones play a key role in SPV dynamics since they can create conditions for advection of air with high vorticity from the SPV region to tropics through the so-called Rossby wave breaking in the stratosphere [McIntyre, Palmer, 1983; Antokhina et al., 2024]. Intensification of the anticyclones causes SPV to deform and decrease and the conditions for sudden stratospheric warmings (SSWs) to develop.

SSW is a sharp weakening of SPV accompanied by a reduction in its area and an increase in the polar stratosphere temperature. During these events, SPV either shifts away from the pole or splits into two (or more) parts, which leads to significant changes in the circulation structure [Lawrence, Manney, 2018; Limpasuvan et al., 2005; Baldwin et al., 2021]. SSWs have a significant impact on tropospheric processes, generating extreme weather events such as changes in circulation and extreme surface temperatures [Baldwin, Dunkerton, 2001; Hitchcock, Simpson, 2014; Kidston et al., 2015; Smith et al., 2018]. The average occurrence rate of SSWs is 0.7 cases per year, and in recent decades there has been a tendency for them to begin earlier [Zorkaltseva et al., 2023].

Mechanisms of SSW formation remain the subject of scientific discussion. The bottom-up hypothesis suggests that SSWs are initiated by amplification of planetary waves from the troposphere, which is linked to atmospheric blocking processes, El Niño, the Madden—Julian oscillation, and snow cover features [Vyatkin et al., 2024; Kandieva et al., 2019; Baldwin et al., 2021]. The top-down hypothesis assumes that SSWs can be caused by internal processes in the stratosphere, including wave-to-medium flux interactions or wave-to-wave nonlinear interactions [Didenko et al., 2019], as well as quasi-biennial equatorial wind oscillations [Holton, Tan, 1980].

In this paper, we examine SSW formation conditions by analyzing changes in the SSW area and the polar stratosphere temperature for the period from 1979 to 2024. Our main concern is with the relationship between these parameters and SSW events, as well as their long-term variability. For the winter periods 2022–2023 and 2023–2024, we have carried out in-depth analysis of SSW dynamics, including conditions preceding SSW and their consequences. The aim of the work is to identify patterns of interaction of SPV with tropospheric anomalies and to determine factors influencing the variability of vortex characteristics in terms of SSW events.

1. DATA AND METHODS

The analysis and calculations have been performed using data from the ECMWF ERA5 climate archive on a 2.5°×2.5° grid [Hersbach et al., 2020]. We analyzed variations in the zonal mean air temperature along 80° N (T) and the zonal mean wind velocity along 60° N (U), which were used as criteria for identifying SSWs. The archive of U and T variations for each winter season from 1979 to 2024 is available at [https://disk.yandex.ru/d/IkG02E1Qb-Uq1g].

Methods of estimating the SPV area can be divided into three main groups depending on the approaches to determining SPV boundaries:

1. Methods using geopotential isolines at pressure levels (for example, 10 hPa) or the latitude of the maximum zonal wind speed. These methods are computationally simple, yet they can oversimplify the boundary during vortex deformation [Schoeberl, Hartmann, 1991].

2. Objective identification methods, including gradient methods and clustering algorithms, make it possible to pinpoint the boundaries. These methods are particularly effective for irregular vortex shapes, but they are computationally difficult [Cámara et al., 2017; Bushra, Rohli, 2019; Kuchar et al., 2024].

3. A method using a potential vorticity (PV) contour on an isentropic surface (equal potential temperature) of 850 K. This method, like type 1 methods, is simple, but it determines the dynamic structure of the vortex [Hoskins et al., 1985; Nash et al., 1996]. Assuming that the maximum potential vorticity gradient is concentrated at the edge of the vortex and neglecting the effects of friction and diabatics, we arrive at a simple model of PV evolution as a conservative value. Since the evolution of such quantities is completely determined by the evolution of their contours, which share different values, the use of PV to find boundaries of the vortex and then to calculate its area is physically justified.

Figure 1 illustrates PV distributions at 850 K (~32 km). Tropical stratosphere areas in the range 0–200 potential vorticity units (pvu), SPV areas in the range 450–700 pvu (and above), as well as mixing areas forming the so-called surf zone are clearly defined. Daily distributions of PV in the middle stratosphere from November to March for 1979–2024 are presented at [https://bit.ly/4fYrC3u].

To determine the polar vortex contour from potential vorticity fields at the level of 850 K, we had to to transform the coordinate system into a Lambert azimuthal equal-area projection with a central point (90° N, 0° E) to minimize the error in determining geometric properties of the desired objects. Polygons for each closed vortex contour were drawn separately for 450 and 500 pvu. Thus, for each level we have obtained a set of polar vortex contours, which may be more than one in the case of SPV splitting. The total area is defined as the sum of areas of all contours for the selected pvu level and date.

To evaluate the SPV stratospheric dynamics and deformation, we also calculated amplitudes of planetary waves with wavenumbers 1 (PV1) and 2 (PV2).

The effect of tropospheric conditions on the SPV dynamics was estimated by analyzing a three-dimensional wave activity vector (WAV), the so-called Plumb vector [Plumb, 1985]. The following relations were used to calculate the Plumb WAV components $\mathbf{F_s}$:

$$\mathbf{F_s} = p\cos\phi \begin{pmatrix} \frac{1}{2a^2\cos^2\phi}\left[\left(\frac{\partial\psi'}{\partial\lambda}\right)^2 - \psi'\frac{\partial^2\psi'}{\partial\lambda^2}\right] \\ \frac{1}{2a^2\cos\phi}\left(\frac{\partial\psi'}{\partial\lambda}\frac{\partial\psi'}{\partial\phi} - \psi'\frac{\partial^2\psi'}{\partial\lambda\,\partial\phi}\right) \\ \frac{2\Omega^2\sin^2\phi}{N^2 a\cos\phi}\left(\frac{\partial\psi'}{\partial\lambda}\frac{\partial\psi'}{\partial z} - \psi'\frac{\partial^2\psi'}{\partial\lambda\,\partial z}\right) \end{pmatrix},$$

where $p = \frac{p_{\text{lev}}}{1000_{\text{mbar}}}$ is the reduced pressure; ψ' is small current function perturbations; ϕ is the latitude; λ is the longitude; $z = -H\log\frac{p_{\text{lev}}}{1000}$ is the altitude; a is the Earth radius; Ω is the angular Earth velocity; N is the Brunt-Väisälä frequency. The calculations utilized climatological geopotential and temperature data (for calculating N) from the ECMWF ERA5 database with a resolution of 2.5°×2.5°×19 levels p_{lev} as initial data. For each node of the grid, we computed $\psi' = \frac{\left(Z - \langle Z_\lambda\rangle\right)g}{f}$, where Z is the geopotential; $\langle Z_\lambda\rangle$ is the geopotential averaged over longitudes; g is the free fall acceleration; f=2ωsinϕ is the Coriolis parameter.
From the data, we quantified the relationship between the SPV area and the polar stratosphere temperature, as well as the SPV dynamics for the two winter seasons.

2. RESULTS

2.1. SPV area

As noted above, the PV contours in the range from 450 to 700 puv visually correlate with SPV. It was necessary to select the contour as the SPV boundary. It is seen (Table 1) that annual variations in the areas of 450 and 500 pvu occur synchronously, with a maximum in December and a minimum in March. On average, the SPV area proved to be larger by 5 million km^2 in the 450 pvu contour than in 500 pvu. We use the 500 pvu contour since qualitative analysis of PV distributions from 1979 to 2024 has shown that the 450 pvu contour is often involved in the surf zone, forming a tail of the vortex [McIntyre, Palmer, 1983], i.e. it is the outer edge of SPV involved in mass exchange with low latitudes.

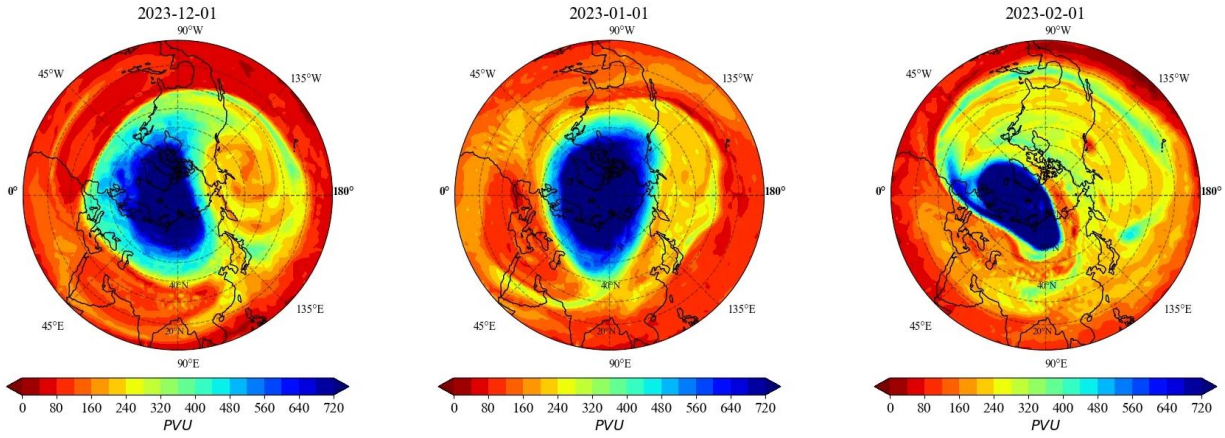

Figure 1. Distributions of PV on December 1, January 1, and February 1, 2022–2023.

Table 1

SPV areas from November to March, as well as the average for the entire period, within the 500 and 450 pvu isolines

SPV area, 10^6 km^2		
Period	500 pvu	450 pvu
March	**15.9**	**20.9**
February	21.9	26.1
January	30.6	34.5
December	**36.0**	**41.5**
November	30.6	36.5
average	27.0	31.9

In Figure 2 are maps of winter PV values averaged over 1979–2024. The location of the stratospheric polar vortex is marked with light blue and blue fills corresponding to values above 500 pvu.

It is evident that by November SPV had already been formed, maximum PV values in the polar stratosphere were observed in December, and there was also an increase in the SPV area. In January–February, the SPV area decreased, which is attributed to the high occurrence rate of SSWs during these months. In March, final SSWs often occurred; moreover, a gradual circulation transition began in this month, causing PV to significantly decrease and the SPV area to be reduced in the polar region (see Figure 2, Table 1).

2.2. SSW

Sudden stratospheric warmings contribute substantially to the SPV dynamics, which is reflected in a reduction in the average vortex area in January relative to December. To analyze in more detail the impact of SSW on SPV, we have examined the winter periods 2022–2023 (Figure 3, *a*, *c*) and 2023–2024 (see Figure 3, *b*, *d*), for which there is a significant difference in the time of SSW onset and intensity and in SPV area dynamics. The first half of the winter 2022–2023 was characterized by the abnormally cold stratosphere. Absolute temperature minima were recorded twice, in November and December, with a slight rise in temperature between them. During these months, the SPV area exceeded the climatic normal, which indicates its enhanced condition. Only in early January 2023, a gradual reduction in the vortex area began, which ended in a minor SSW later this month. However, the next month saw a major SSW with maximum February temperature for the entire period considered.

No extreme variations in stratospheric parameters occurred during the winter season 2023–2024. Temperature fluctuations began to appear at the end of November, and December turned out to be warmer than the climatic normal. The SPV area started to decrease in December. A feature of the winter 2023–2024 was a large number of sudden stratospheric warmings.

Four SSWs were recorded, three of which were accompanied by a reversal of the zonal wind at midlatitudes and hence were classified as major, although in two of them the wind reversal was minimum (1–2 m/s) and lasted only a few days.

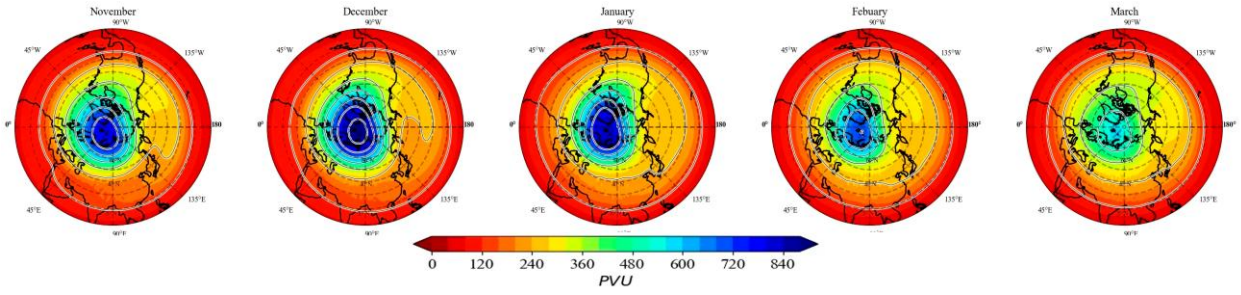

Figure 2. Long-term average potential vorticity at 850 K from November to March

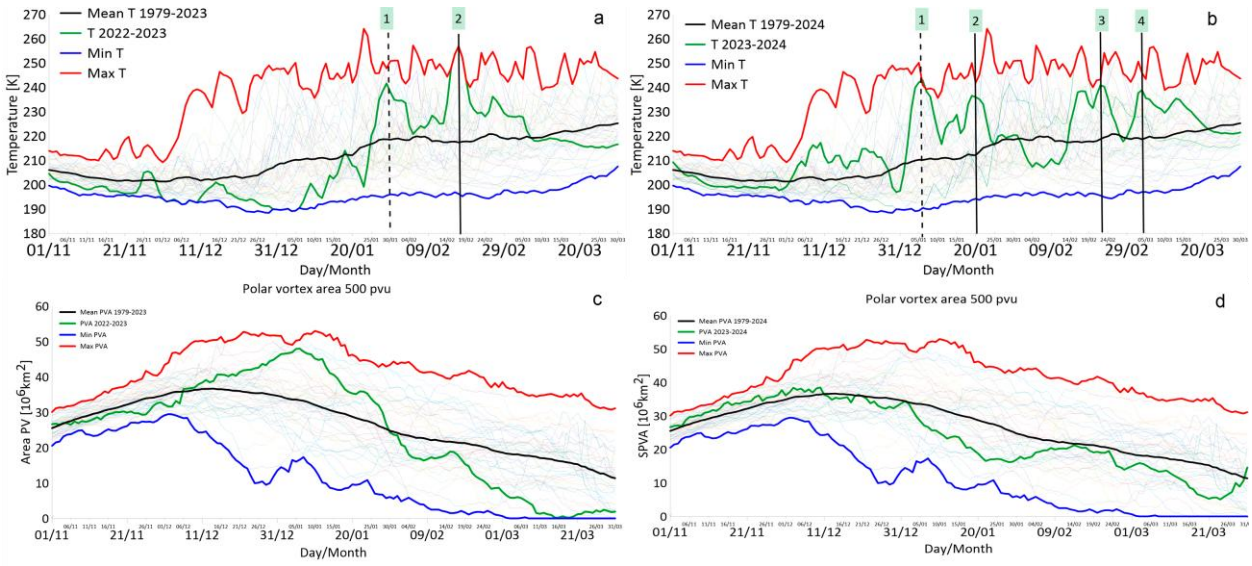

Figure 3. Variations in the polar stratosphere temperature (*a*, *b*) and the SPV area (*c*, *d*) from November to March 2022–2023 (*a*, *c*) and 2023–2024 (*b*, *d*); vertical lines mark the days of maximum temperature for minor (dashed line) and major (solid line) SSW. The red line indicates maximum values; the blue line, minimum values; and the black line, averages for the period from 1979 to 2024. Green lines show averages for the winters 2022–2023 (left) and 2023–2024 (right)

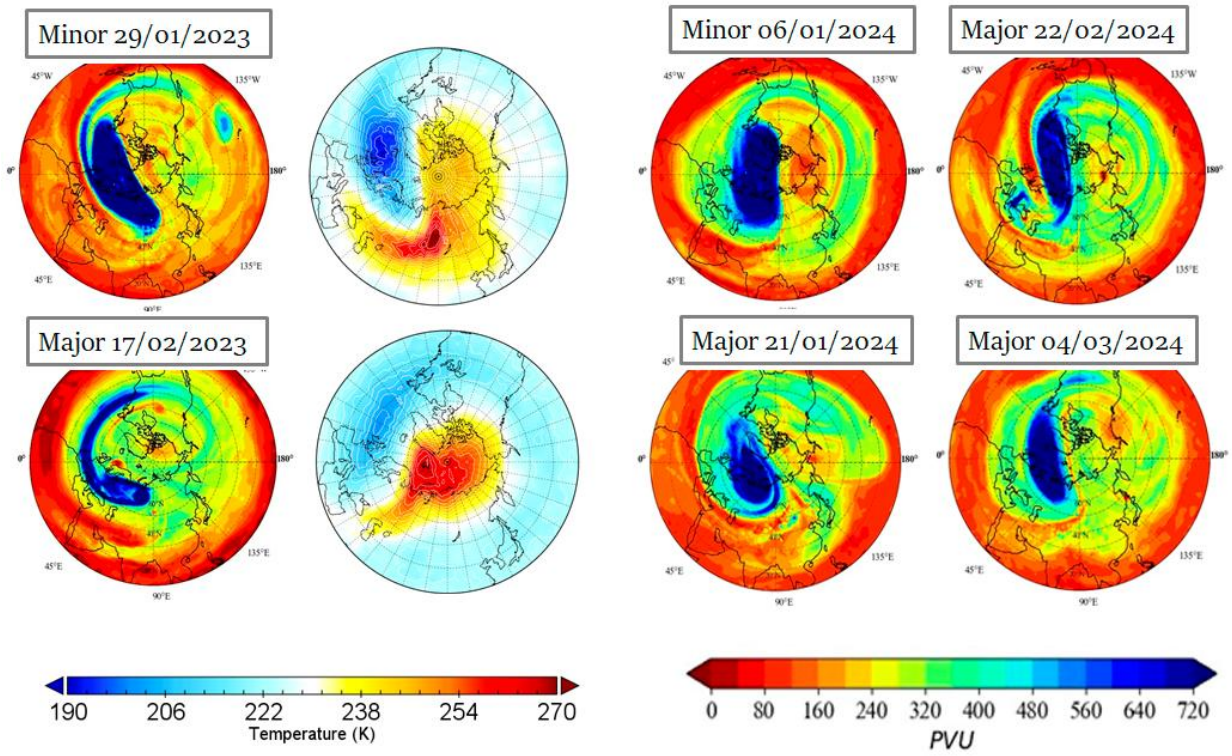

Figure 4. Distributions of potential vorticity at 850 K and temperature at 10 hPa on the day of SSW maxima

Despite four SSWs, amplitude of changes in such key parameters as temperature and SPV area remained within the climatic normal. This contrasts with the winter 2022–2023, which began with extremely low temperatures and a significant increase in the SPV area, and ended with record-breaking warming and a decrease in the vortex area relative to the climatic normal. The differences in the dynamics of the SPV parameters during the two winter seasons suggest that the mechanisms behind their variability are complex.

By the type of polar vortex deformation, all SSWs in the winters 2022–2023 and 2023–2024 are classified as vortex displacement (Figure 4). Two SSWs in 2022–2023 and four SSWs in 2023–2024 demonstrated SPV displacement to Europe and the Atlantic. All the SSWs took place in the Eastern Hemisphere, which corresponds to the most frequently observed scenario of SSW development.

2.3. Polar stratosphere temperature and SPV area

Analysis of variations in the polar stratosphere temperature and the SPV area during the two winter periods

has shown that these parameters are inversely related: with a large size of SPV, the polar stratosphere has low temperatures, and vice versa. The same pattern can be traced for previous winter seasons. Figure 5 illustrates long-term variations in SPV area anomalies from 1979 to 2024. Temperature anomalies in the polar stratosphere are depicted by isolines, and the days of SSW onset are marked with blue rhombuses. This approach allows us to visualize the relationship between key SPV parameters and SSW events, as well as to assess their impact on long-term circulation trends in the stratosphere.

It is apparent that there are moments of temperature increase, which are followed by a vortex area decrease and SSW occurence. For example, in the late 1990s and early 2000s, abnormally small vortex areas and early SSWs were observed for 5–6 years. Later, there was a gradual shift in SSW dates to a more familiar time — midwinter. An equally interesting feature is the occurrence of abnormally large vortices in the first half of winter and in March since 2007. This phenomenon is often considered in the literature as an extreme vortex event [Lawrence et al., 2020; Baldwin and Dunkerton, 2001], which was also typical of the winter period 2022–2023.

If we look at the trends in SPV and temperature variations averaged over the winter periods, we can see that the temperature decreased and the SPV area increased from 1979 to 2024 (Figure 6), yet monthly temperature and SPV variations are not so uniform. March is generally responsible for the average winter trend; it exhibits a significant decrease in temperature and an increase in vortex area. In January, the reverse is true — an increase in temperature and a decrease in SPV area.

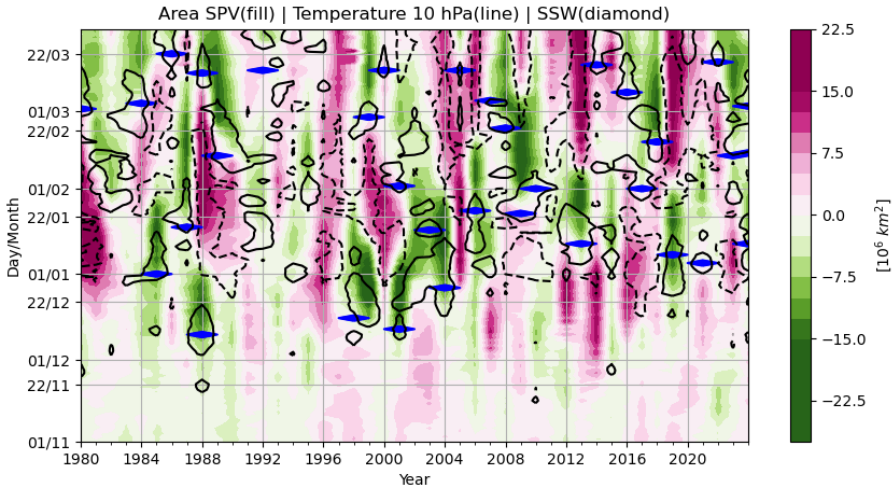

Figure 5. Anomalies in SPV area (fill) and temperature at 10 hPA (solid line — +10 K, dashed line — –10 K); blue rhombuses mark the days of SSW onset

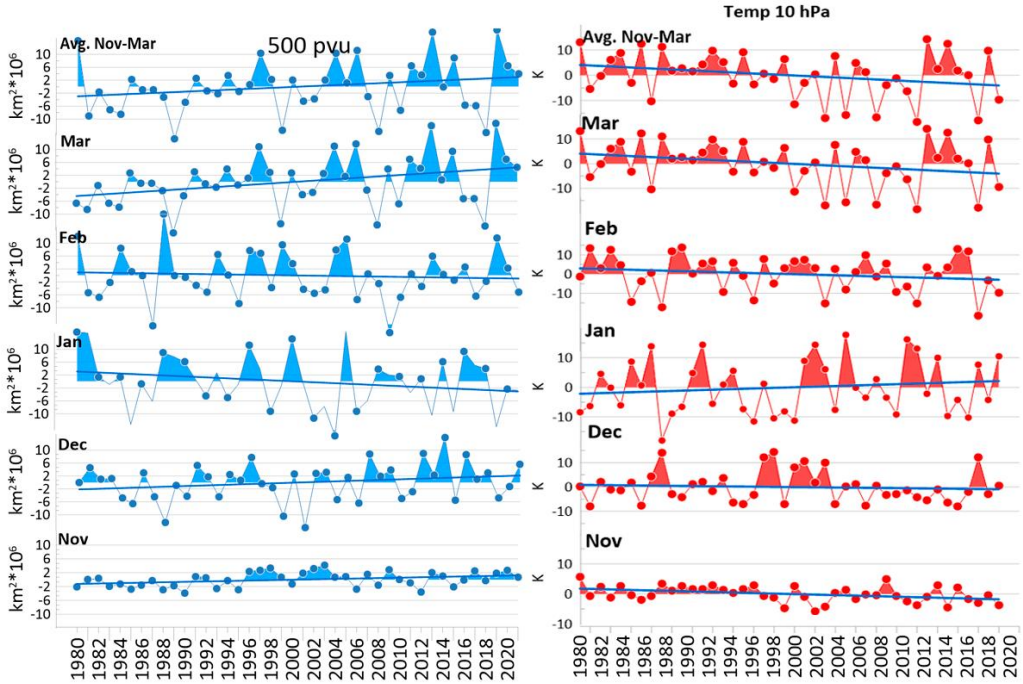

Figure 6. Long-term variations of anomalies in SPV area (*a*) and temperature at 10 hPA (*b*)

Analyzing the regression dependence of the average long-term values of the vortex area and the polar stratosphere temperature (Figure 7), it is impossible not to note an inflection in December. Up to this point, the vortex area increases and the temperature decreases, but after December the vortex area begins to go down and the temperature goes up. The correlation coefficients between the SPV area and the temperature turned out to be high (Table 2), although they are slightly lower in December and February. In December, this is likely due to the very inflection that can occur at different times in different years. In February, the low correlation coefficient is explained by the high occurrence rate of SSWs, which violate the inverse relationship since the temperature changes much faster than the vortex area (see Figure 3).

Table 2

Correlation coefficients between polar stratosphere temperature and SPV area

Correlation coefficient			
Period	1979–2024	2022–2023	2023–2024
March	–0.98	0.82	
February	–0.30	0.15	
January	–0.95	–0.93	0.1
December	–0.62	–0.10	0.1
November	–0.94	0.10	0.0
average	–0.91	–0.68	–0.6

If we look at the relationship between the SPV area and the temperature for specific winters, the dependence is not so pronounced. The correlation coefficients are much lower than the long-term average. When comparing the two winters, we can note that the transition from the increasing area — decreasing temperature pattern to the decreasing area — increasing temperature one in 2022–2023 occurred not in December, as is usually the case, but a month later. In 2023–2024, due to numerous SSWs, the regression looks more chaotic; nevertheless, the transition to the decreasing area — increasing temperature pattern took place in December.

2.4. Planetary waves

The differences in the behavior of SPV and stratosphere temperature during the two winter seasons can be explained by planetary wave activity with wavenumbers 1 and 2 (PV1 and PV2 respectively) on the isobaric surface of 10 hPa along the latitudinal circle of 60° N (Figure 8). Since there were SSWs with vortex displacement in both seasons, the main focus should be on PV1. In November–December 2022, the amplitude of PV1 was below normal, but since January 2023 it significantly exceeded it. Already since December, significant differences between the winters can be observed: in 2023–2024, the PV1 amplitude was much higher than the climatic normal from December to March. In winter 2022–2023, despite the increase in PV1 activity in January, the polar vortex remained stable until mid-February (Figure 9). Note, however, that the increased wave activity in January 2023 prepared the conditions for major SSW in February 2023. On average for the winter (Figure 8, right)

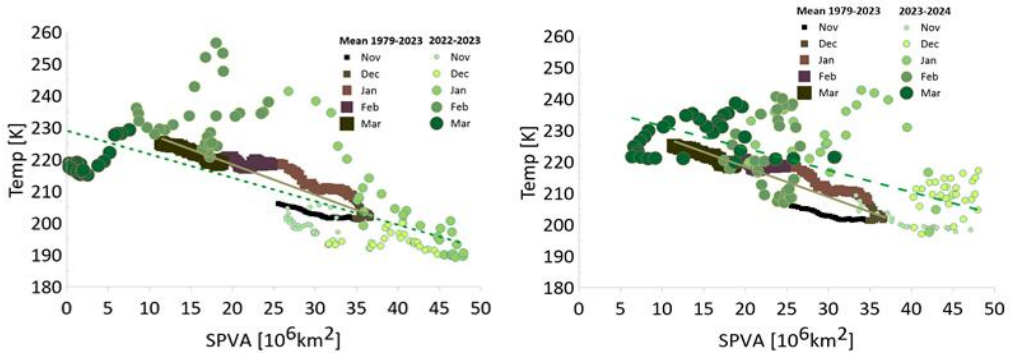

Figure 7. Regression dependence of temperature on SPV area: brown palette — averages for 1979–2024, green palette — winters 2022–2023 (*a*) and 2023–2024 (*b*)

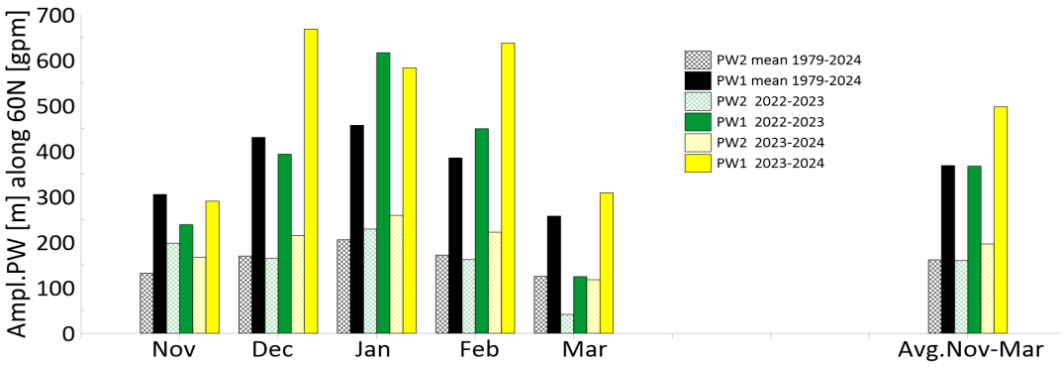

Figure 8. Average amplitudes of PV1 (solid fill) and PV2 (cross-hatching) during the winter periods 2022–2023 (green) and 2023–2024 (yellow), as well as from 1979 to 2024 (black and gray)

we can see that increased amplitudes of PV1 led to a smaller vortex area in 2023–2024, whereas in 2022–2023 the vortex area remained close to normal. At the same time, within the winter period, SPV area variations were much more significant in 2022–2023 than in 2023–2024. Thus, the first half of the winter 2022–2023 was characterized by harsh conditions and large SPV, followed by record-breaking warming in February and a vortex decrease after which the vortex remained small until the seasonal circulation transition in the stratosphere.

2.5. Tropospheric forcing

Differences between the winters 2022–2023 and 2023–2024 are observed not only in the stratosphere, but also in the mid-latitude troposphere, which naturally affects the distribution of wave activity fluxes (WAFs) in the atmosphere. This is shown by zonal mean vertical Plumb WAFs along 60° N, which characterize planetary wave propagation (Figure 10). It is obvious (see Figure 10) that an upward flux prevails at midlatitudes, yet downward WAF was observed in the second half of December 2022. In contrast, a quasi-periodic upward flux was recorded throughout the winter 2023–2024. Moreover, the plots for 2023–2024 show that upward WAF remains quite intense in the lower troposphere to ~500 hPa. If this flux manages to penetrate into the upper troposphere, it often continues to propagate into the stratosphere, so it is worth examining features of the spatial distribution of vertical WAF at the boundary between the troposphere and the stratosphere (~100 hPa).

To begin with, let us examine the climatic distribution of the WAF vertical component in winter (Figure 11). Wave fluxes have been studied in detail in [Jadin, Zyulyaeva, 2010; Zyulyaeva, Zhadin, 2009]. According to these studies, planetary waves penetrate from the troposphere into the stratosphere mainly over the north of Eurasia, whereas weak downward fluxes are recorded near the Labrador Peninsula and Southern Greenland. This phenomenon has been called the stratospheric bridge. Intensification of penetration of planetary waves into the stratosphere in December leads to significant changes in its dynamics, creating preliminary conditions for the occurrence of SSW in January.

To analyze the stratospheric bridge, we have constructed maps of anomalies of vertical WAFs, averaged over the winters 2022–2023 and 2023–2024. Figure 12 exhibits height–latitude sections of the WAF vector from November to March, which show significant differences in WAF at the beginning of the winter season, especially in November and December, between the years considered. In November 2022, an ascending branch of the bridge did not form over Asia, and in December a positive anomaly was detected only in part of this region. Figure 12 demonstrates that the differences in the dynamics of the stratospheric vortex area between the two winters are explained by anomalies in the wave activity flux from the troposphere. The WAF distributions in January 2023 and December 2023 are similar.

Thus, the formation of the large and cold stratospheric vortex during the winter season 2022–2023 was linked to the late formation of upward WAF from the troposphere.

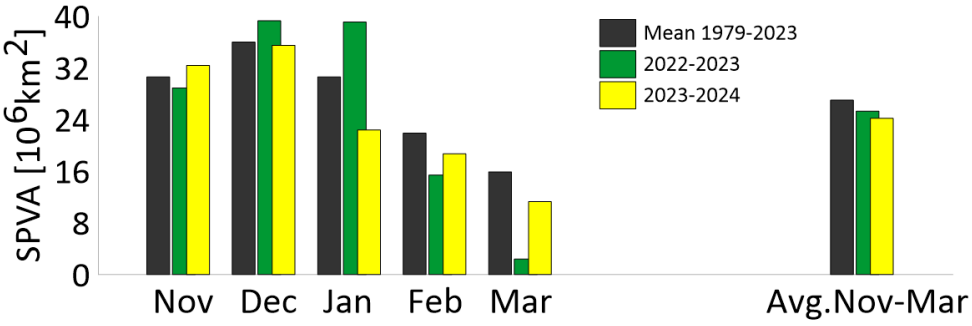

Figure 9. Average SPV areas: black — long-term, green — for the winter 2022–2023, yellow — for the winter 2023–2024.

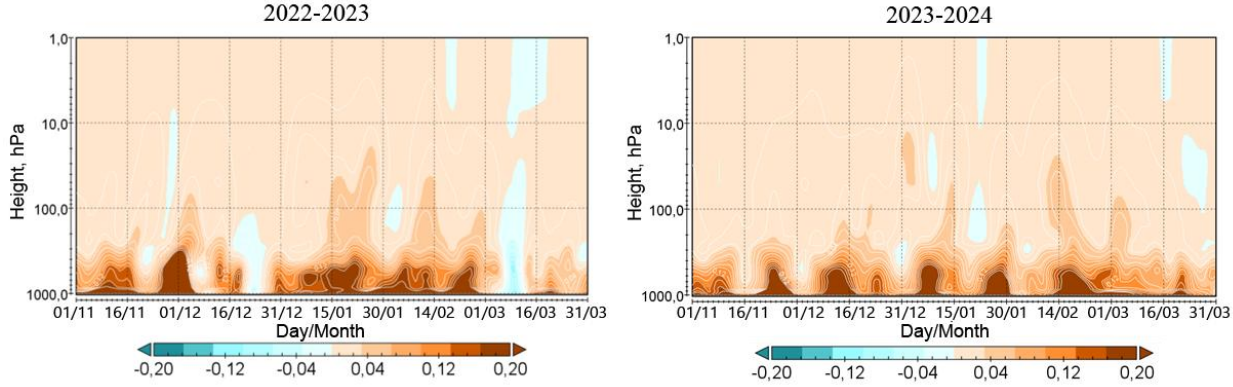

Figure 10. Plumb wave activity flux vertical component zonally averaged along 60° N from November 1, 2022 to March 1, 2023 (*a*) and from November 1, 2023 to March 1, 2024 (*b*)

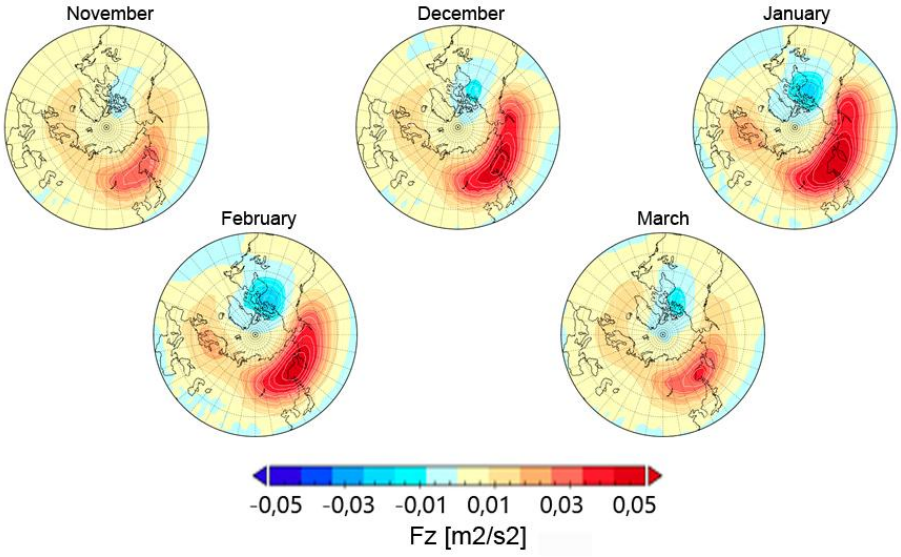

Figure 11. Spatial distribution of the monthly average climatic vertical component of the Plumb wave activity flux

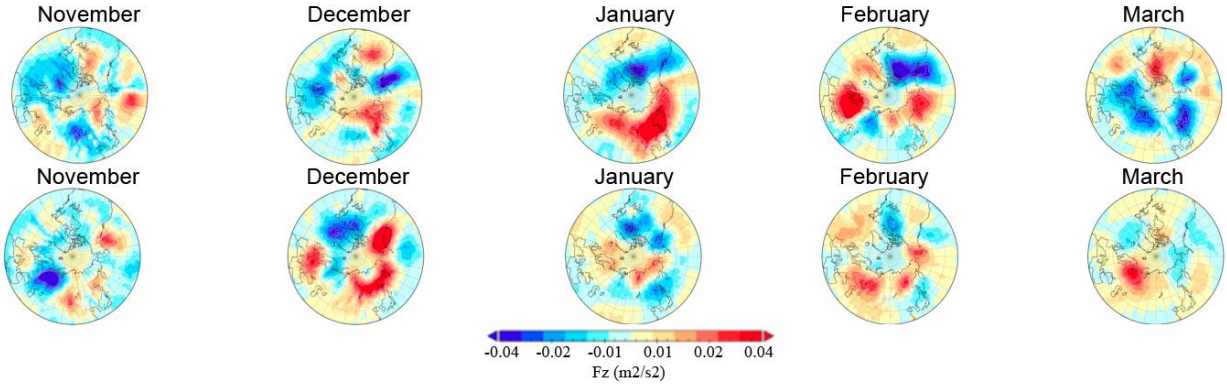

Figure 12. Fill — maps of anomalies of vertical WAFs averaged for the winters 2022–2023 (top) and 2023–2024 (bottom). Height–latitude sections represent WAF vectors

3. DISCUSSION

Comparing the two winter periods has allowed us to identify differences that were observed not only in the stratosphere, but also in the troposphere. Nonetheless, some aspects of the winter stratosphere remained unaddressed, for example, meridional heat fluxes, residual circulation, El Niño, quasi-biennial equatorial wind cyclicity, Madden—Julian oscillation (MJO), etc. The winter periods 2022–2023 and 2023–2024 have been analyzed in other works, for example, [Vargin et al., 2024; Lu et al., 2023; Qian et al., 2024]. Below we will focus on some of the results of these works. Vargin et al. [2024] have observed that the cold and stable polar vortex in the first half of the winter 2022–2023, we have also examined in our work, caused the largest volume of polar stratospheric clouds on record since 1980. The minor SSW in January 2023 was accompanied by a record meridional heat flux in the lower stratosphere and significant changes in the residual meridional circulation. Changes in the WAF configuration after the January SSW contributed to the formation of a major SSW in February, which is confirmed by the results of this work (see Figure 8).

Lu et al. [2023] have studied the stratosphere-troposphere coupling in the winter 2022–2023 and have found that the minor SSW in January 2023 had a response in the lower troposphere, but the downstream impact was weak. As we do in this paper, Lu et al. [2023] attribute the major SSW in February 2023 to a critical increase in the PV1 amplitude, but observe that the major SSW caused significant cold anomalies throughout North America until the end of March. Among other things, the authors noted that La Niña conditions contributed to the intensification of planetary waves. Significant ice loss in the Barents Sea and the Laptev Sea was another factor triggerring the SPV disturbances in January–February 2023. The development of MJO phases 4–6 two weeks before the major SSW also had an effect.

Qian et al. [2024] have also attributed the three major SSWs of the winter season 2023–2024 to the polar vortex displacement due to the PV1 dynamics. Qian et al. [2024] have found that stratospheric disturbances propagated to the lower troposphere during SSW, causing cold waves in all continental regions of the Northern Hemisphere. They also observed an intensification of the meridional residual circulation, which transferred a large amount of water vapor into the tropical stratosphere, which had a significant impact on the composition of the stratosphere.

Thus, the results of our study, being in agreement with the results of other researchers, expand and complement the set of factors influencing the dynamics of the winter stratosphere. In contrast to the above works dealing with the SSW effects in weather conditions, we have focused on the role of tropospheric forcing in the dynamics of the stratosphere. We attribute the presence of cold and large-scale SPV in the winter 2022–2023 to a delay of a month in the formation of the stratospheric bridge compared to the winter 2023–2024. The winter season 2022–2023 is a prominent example of the continuation of the trend, which emerged in the late 1990s, toward the formation of extremely large SPVs in the first half of the winter and major SSWs in the second half. At the same time, the minor SSW on January 6, 2024 contributed to the trend for an increase in the occurrence rate of early major SSWs.

In the context of our study, the results obtained by Zou and Zhang [2024] may be useful in explaining the trend toward the formation of extremely large SPVs in the first half of winter and strong SSWs in the second half. The loss of sea ice in the Arctic can enhance the upward wave activity from the troposphere, with the maximum positive surface temperature anomalies observed in the Kara and Barents Seas, where the warm Arctic – cold Eurasia pattern is formed [Zhang et al., 2018]. This might alter the configuration of WAF spatial distribution, i.e. WAF in the troposphere remains high, but is localized away from the ascending branch of the stratospheric bridge. This aids in extending and increasing the SPV area at the beginning of winter. As a result, SSWs can occur in the second half of winter, with high amplitudes, as we observed in the winter season 2022–2023. The above considerations will serve as a starting point for our further research. The high year-to-year variability in processes in the winter stratosphere, we have noted in this work, determines the relevance of further study of the SPV dynamics in the context of long-term changes.

CONCLUSION

We have examined variations in the stratospheric polar vortex (SPV) area, the high-latitude stratosphere temperature, the amplitude of planetary waves, and Plumb wave activity fluxes from November to March for the two winter seasons 2022–2023 and 2023–2024 against the background of long-term averages from 1979 to 2024. In 2022–2023, the SPV area significantly exceeded the climatic normal in December and January, and it decreased a month later than the climatic normal. This was accompanied by extremely low temperatures of the polar stratosphere in the first half of the winter and record-breaking hot sudden stratospheric warming in the second half of the winter. During the winter period 2022–2023, there were two SSWs — a minor one at the end of January, and a major one in mid-February. The long-term increase in the vortex area and the later occurrence of major SSW in the winter 2022–2023 relative to 2023–2024 were associated with decreased wave activity in the stratosphere in the first half of winter, which was caused by wave activity anomalies in the troposphere. In the winter period 2023–2024, there were no extreme values of SPV area and temperature; however, during the winter period there were four SSWs, three of which were major. On average, the polar stratosphere temperature is inversely proportional to the stratospheric polar vortex area. The inverse correlation can be significantly disrupted in some years, as, for example, happened in 2023–2024 due to the large number of SSWs.

Noteworthy in the changes in the parameters considered are the late 1990s and the early 2000s, where abnormally low vortex areas and early SSWs were recorded for 5–6 years. An equally interesting feature is the occurrence of abnormally large vortices in the first half of winter since 2007. If we look at the SPV and temperature trends averaged over the winter period, we can see that the temperature decreased and the SPV area increased from 1979 to 2024. However, monthly variations in temperature and SPV are not so uniform. March is generally responsible for the average winter trend, which is characterized by a significant decrease in the temperature and an increase in the vortex area. In January, a reverse trend is observed — a slight increase in the temperature against the background of a decrease in the SPV area. The winter season 2022–2023 continues the trend toward the formation of extremely large SPVs in the first half of the winter and strong SSWs in the second half. At the same time, the minor SSW on January 6, 2024 contributed to the trend for increasing occurrence rate of early SSWs. The high year-to-year variability of the processes in the winter stratosphere necessitates further study of the SPV dynamics in the context of long-term changes.

Analysis and interpretation of the results were carried out under RSF project No. 22-7710008. Data processing and storage were financially supported by the Russian Ministry of Science and Higher Education (Subsidy No. 075-GZ/Ts3569/278).

REFERENCES

Andrews D., Taylor F., McIntyre M. The influence of atmospheric waves on the general circulation of the middle atmosphere. *Philosophical Transactions of the Royal Society of London. Series A: Mathematical, Physical and Engineering Sciences*. 1987, vol. 323, iss. 1575, pp. 693–705. DOI: 10.1098/rsta.1987.0115.

Antokhina O.Yu., Gochakov A.V., Zorkaltseva O.S., Antokhin P.N., Krupchatnikov V.N. Rossby wave breaking in the stratosphere: Part I — Climatology and long-term variability. *Atmospheric and Oceanic Optics*. 2024, vol. 37, no. 4, pp. 514–52. DOI: 10.1134/S1024856024700696

Baldwin M.P., Dunkerton T.J. Stratospheric harbingers of anomalous weather regimes. *Science*. 2001, vol. 294, pp. 581–584.

Baldwin M., Ayarzaguena B., Birner T., Butchart N., Butler A., Charlton-Perez A., Sudden stratospheric warmings. *Rev. Geophys*. 2021, vol. 59. DOI: 10.1029/2020RG000708.

Bushra N., Rohli R.V. An objective procedure for delineating the circumpolar vortex. *Earth and Space Science*. 2019, vol. 6, no. 5, pp. 774–783. DOI: 10.1029/2019EA000590.

Cámara A., Albers J., Birner T., Garcia R., Hitchcock P., Kinnison D., Smith A. Sensitivity of sudden stratospheric warmings to previous stratospheric conditions. *J. Atmos. Sci*. 2017, vol. 74, no. 9, pp. 2857–2877. DOI: 10.1175/JAS-D-17-0136.1.

Didenko K.A., Ermakova T.S., Koval A.V., Pogoreltsev A.I. Diagnostics of nonlinear interactions of stationary planetary waves. *Scientific notes of the Russian State Hydrometeorological University*. 2019, no. 56. DOI: 10.33933/2074-2762-2019-56-19-29. [In Russian].

Hersbach H., Bell B., Berrisford P., Hirahara S., Horányi A., Muñoz-Sabater J., et al. The ERA5 Global Reanalysis. *Quarterly Journal of the Royal Meteorological Society*. 2020, vol. 146, pp. 1999–2049. DOI: 10.1002/qj.3803.

Hitchcock P., Simpson I.R. The downward influence of stratospheric sudden warmings. *J. Atmos. Sci.* 2014, vol. 71, pp. 3856–3876. DOI: 10.1175/JAS-D-14-0012.1.

Holton J.R., Tan H.-C. The influence of the equatorial quasi-biennial oscillation on the global circulation at 50 mb. *J. Atmos. Sci*. 1980, no. 37, pp. 2200–2208. DOI: 10.1175/1520-0469(1980)037<2200:TIOTEQ>2.0.CO;2.

Hoskins B.J., McIntyre M.E., Robertson A.W. On the use and significance of isentropic potential vorticity maps. *Quarterly Journal of the Royal Meteorological Society*. 1985, vol. 111, no. 470, pp. 877–946. DOI: 10.1002/qj.49711147002.

Jadin E.A., Zyulyaeva Yu.A. Interannual variations in the total ozone, stratospheric dynamics, extratropical SST anomalies and predictions of abnormal winters in Eurasia. *International Journal of Remote Sensing*. 2010, vol. 31, pp. 851–866. DOI: 10.1080/01431160902897874.

Kandieva K.K., Aniskina O.G., Pogoreltsev A.O., Zorkaltseva O.S., Mordvinov V.I. Effect of Madden–Julian oscillation and quasi-biennial oscillation on the dynamics of extratropical stratosphere. *Geomagnetism and Aeronomy*. 2019, vol. 59, no. 1, pp. 105–114. DOI: 10.1134/S0016793218060063.

Kidston J., Scaife A., Hardiman S., Mitchell D., Butchart N., Baldwin M., Gray L. Stratospheric influence on tropospheric jet streams, storm tracks and surface weather. *Nature Geosci*. 2015, vol. 8, pp. 433–440. DOI: 10.1038/ ngeo2424.

Kuchar A., Öhlert M., Eichinger R., Jacobi C. Large-ensemble assessment of the Arctic stratospheric polar vortex morphology and disruptions. *Weather and Climate Dynamics*. 2024, vol. 5, no. 3, pp. 895–912. DOI: 10.5194/wcd-5-895-2024.

Lawrence Z., Manney G. Characterizing stratospheric polar vortex variability with computer vision techniques. *J. Geophys. Res.: Atmos*. 2018, vol. 123, no. 3, pp. 1510–1535. DOI: 10.1002/2017JD027556.

Lawrence Z., Perlwitz J., Butler A., Manney G., Newman P., Lee S., Nash E. The remarkably strong Arctic stratospheric polar vortex of winter 2020: Links to record-breaking Arctic oscillation and ozone loss. *JGR Atmosphere*. 2020, vol. 125, no. 22. DOI: 10.1029/ 2020JD033271.

Limpasuvan V., Hartmann D. L., Thompson D. W., Jeev K., Yung Y. L. Stratosphere-troposphere evolution during polar vortex intensification. *Geophys. Res.* 2005, vol. 110. DOI: 10.1029/ 2005JD006302.

Lu Q., Rao J., Shi C., Ren R., Liu Y., Liu S. Stratosphere-troposphere coupling during stratospheric extremes in the 2022/23 winter. *Weather Climat. Extrem.* 2023, vol. 42. DOI: 10.1016/ j.wace.2023.100627.

McIntyre M.E., Palmer T.N. Breaking planetary waves in the stratosphere. *Nature*. 1983, vol. 305, no. 5935, pp. 593–600.

Nash E., Newman P., Rosenfield J., Schoeberl M. An objective determination of the polar vortex using Ertel's potential vorticity. *J. Geophys. Res.* 1996, vol. 101, pp. 9471–9478. DOI: 10.1029/96JD00066.

Plumb R.A. On the three-dimensional propagation of stationary waves. *J. Atmos. Sci.* 1985, vol. 42, no. 3, pp. 217–229. DOI: 10.1175/15200469(1985)042<0217:ottdpo>2.0.co;2.

Qian L. Rao J., Shi C., Liu S. Enhanced stratosphere-troposphere and tropics-Arctic couplings in the 2023/24 winter. *Nature. Communications Earth & Environment*. 2024, vol. 5. DOI: 10.1038/s43247-024-01812-x.

Schoeberl M.R., Hartmann D.L. The dynamics of the stratospheric polar vortex and its relation to springtime ozone depletions. *Science*. 1991, vol. 251, no. 4989, pp. 46–52. DOI: 10.1126/science.251.4989.46.

Smith K., Polvani L., Tremblay L. The impact of stratospheric circulation extremes on minimum Arctic sea ice extent. *J. Climate*. 2018, vol. 31, no. 18, pp. 7169–7183. DOI: 10.1175/JCLI-D-17-0495.1.

Vargin P.N., Koval A.V., Guryanov V.V., Kirushov B.M. Large-scale dynamic processes during the minor and major sudden stratospheric warming events in January–February 2023. *Atmos. Res.* 2024, vol. 308. DOI: 10.1016/j.atmosres.2024.107545.

Vyatkin A.N., Zorkaltseva O.S., Mordvinov V.I. Influence of El Niño on parameters of the middle and upper atmosphere over Eastern Siberia according to reanalysis and model data in winter. *Solar-Terrestrial Physics*. 2024, vol. 10, iss. 1, pp. 40–48. DOI: 10.12737/stp-101202406.

Zhang P., Wu Y., Simpson I., Smith K., Zhang X., De B., Callaghan P. A stratospheric pathway linking a colder Siberia to Barents-Kara Sea sea ice loss. *Sci. Adv*. 2018, vol. 4, no. 7. DOI: 10.1126/sciadv.aat6025.

Zorkaltseva O. S., Antokhina O. Yu., Antokhin P. N. Long-term variations in parameters of sudden stratospheric warmings according to ERA5 reanalysis data. *Atmospheric and Oceanic Optics*. 2023, vol. 36, no. 4, pp. 370–378. DOI: 10.1134/S1024856023040206.

Zou C., Zhang R. Arctic Sea ice loss modulates the surface impact of Autumn Stratospheric Polar Vortex stretching events. *Geophys. Res. Lett*. 2024, vol. 51, no. 3. DOI: 10.1029/2023GL107221.

Zyulyaeva Yu.A., Zhadin E.A. Analysis of three-dimensional Eliassen-Palm fluxes in the lower stratosphere. *Russ. Meteorol. Hydrol*. 2009, vol. 34, no. 8, pp. 483–490.

URL: https://disk.yandex.ru/d/IkG02E1Qb-Uq1g (accessed March 10, 2025).

URL: https://bit.ly/4fYrC3u (accessed March 10, 2025).

Original Russian version: Zorkaltseva O.S., Antokhina O.Yu., Gochakov A.V., Artamonov M.F., published in Solnechno-zemnaya fizika. 2025, vol. 11, no. 2, pp. 89–99. DOI: 10.12737/szf-112202508.

How to cite this article

Zorkaltseva O.S., Antokhina O.Yu., Gochakov A.V., Artamonov M.F. Evolution of the stratospheric polar vortex as evidenced by the winters 2022–2024. *Sol.-Terr. Phys*. 2025, vol. 11, iss. 2, pp. 78–87. DOI: 10.12737/stp-112202508.